Structural Chemistry (2021) 32:2283–2290
https://doi.org/10.1007/s11224-021-01803-0

ORIGINAL RESEARCH

Fullerenes C_{100} and C_{108}: new substructures of higher fullerenes

Ayrat R. Khamatgalimov[1] · Tatiana P. Gerasimova[1] · Timur I. Burganov[1] · Valeri I. Kovalenko[1]

Received: 14 April 2021 / Accepted: 15 June 2021 / Published online: 28 June 2021

Abstract

Based on our approach of theoretical modeling of the fullerene molecule electronic structures, an analysis of the molecular structures of isolated pentagon rule (IPR) isomer 450 (D_5) of fullerene C_{100} and IPR isomer 1771 (D_2) of fullerene C_{108} has been carried out. For the first time, the data about the distributions of single, double, and delocalized π-bonds in studied isomer molecules as well as their molecular formulas are presented. It is revealed that isomer 450 (D_5) of fullerene C_{100} contains two substructures from condensed phenalenyl-radicals at the poles of the molecule (i.e., has an open electronic shell), whereas isomer 1771 (D_2) of fullerene C_{108} has a closed electronic shell and contains substructure from condensed coronenes at the equator of the molecule. Their stabilities are evaluated in accordance with local strains in the molecules and/or the presence of radical substructures.

Keywords Structural formula · Substructure · Othrene · Radical · Overstrain

Introduction

The study of higher fullerenes is quite complicated due to their very low abundance in the fullerene soot and the presence of hundreds of topologically possible isomers with rather lower symmetries that obey the isolated pentagon rule (IPR). IPR suggests that the fullerene molecule with abutting pentagons is unstable [1, 2]. Theoretical investigations of the structures of large fullerenes and their isomers become necessary to analyze experimental results, to determine the structure and stability of isomers, and to predict new structures. Among the other higher fullerenes C_n ($n > 60$), the theoretical information on C_{100} and C_{108} fullerenes is very limited.

For C_{100}, 450 possible molecular geometries satisfy the IPR [3]. However, to date, there is no C_{100} isomers that have been isolated and characterized as an empty cage; they only have been registered by mass spectrometry. According to theoretical calculations, isomer 449 (D_2) is the most stable one followed by isomers 18 (C_2), 173 (C_1), 174 (C_2), 425 (C_1), 440 (C_2), 442 (C_2), in different orders depending on the used theoretical level [4–8]. Besides, considerable temperature effects on the stability are found so that not only the ground-state 449 (D_2) isomer but also several other structures (18 (C_2), 426 (C_1), 425 (C_1), 442 (C_2), 148 (C_1)) are significantly populated within a wide temperature interval [5]. Nevertheless, several isomers of fullerene C_{100} have been identified as various derivatives (exohedral and endohedral).

For the first time, C_{100} was confirmed experimentally as an exohedral $C_{100}Cl_{12}$ with a molecule of unstable isomer 1 (D_{5d}) with a nanotubular shape [9]. Isomers 18 (C_2), 425 (C_1), and 417 (C_{2v}) of C_{100} were also obtained as chloro derivatives whose structures were identified by X-ray analysis [10]. Isomers 425 (C_1) and 18 (C_2) were also identified as C_1–$C_{100}(425)Cl_{22}$ and C_2–$C_{100}(18)Cl_{28/30}$ compounds, respectively, with retained IPR cage connectivities. In contrast, isomer 417 (C_{2v}) has been isolated as C_s–$C_{100}Cl_{28}$ which loses a C_2 fragment, resulting in the nonclassical C_1–$C_{98}Cl_{26}$ with a heptagon in the carbon cage. The computations showed that this isomer originates presumably from isomer 603 (C_1) of fullerene C_{102}, which undergoes the skeletal transformations, including chloride formation, C_2 elimination, and SW transformation [11]. A rather stable isomer 18 (C_2) was also indirectly confirmed as the most probable starting fullerene, whose skeletal transformations lead to obtaining of the nonclassical exohedral $C_{96}Cl_{20}$ and $C_{94}Cl_{22}$ with three and one heptagons, respectively [12, 13].

In contrast to the empty C_{100} fullerenes, endohedral derivatives demonstrate completely different relative stabilities. Thus, IPR isomer 450 (D_5) was theoretically predicted to be

✉ Ayrat R. Khamatgalimov
ayrat_kh@iopc.ru

[1] Arbuzov Institute of Organic and Physical Chemistry, FRC Kazan Scientific Center, Russian Academy of Sciences, 8 Arbuzov Street, Kazan 420088, Russia

the most energetically advantageous C_{100} cage for the fullerenes with endohedral atoms able to donate up to six electrons to the carbon cage. [8, 14, 15] These theoretical findings were later confirmed when $La_2@C_{100}(450)$ had been isolated and established by X-ray analysis [16]. It should be noted that this isomer is one of the most unstable and theoretical calculations predict for it extremely low HOMO-LUMO gap close to zero [5]. The isomer 450 (D_5) was also found in the crystal structure of endohedral carbide cluster metallofullerene $La_2C_2@C_{100}$ [17]. Yang and Dunsch reported the preparation of $Dy_2@C_{100}$ with two metal atoms inside the fullerene cage [18]. They suggested that the most possible hosts are presented by the most stable empty-cage isomers of C_{100} [18]. However, they ignored the charge transfer between the encapsulated metal atoms and the fullerene cage. The role of the latter has been emphasized by Valencia, Rodríguez-Fortea, and Poblet, who found that the isomer 450 (D_5) was an unusually promising candidate [19]. It was also revealed that this cage provides maximal separation between the pentagons, representing the sites of negative charge localization in the fullerene anions [20, 21].

Even fewer studies are devoted to fullerene C_{108}. For C_{108}, 1799 possible molecular geometries satisfy the IPR [3]. Similar to fullerene C_{100}, to date among them, no C_{108} isomers have been isolated and characterized as an empty cage. According to theoretical calculations, isomer 1771 (D_2) is one of the most stable (with a significant HOMO−LUMO gap) among 1799 IPR isomers; thus, this isomer is likely to coexist in the soot and hard to separate experimentally [7]. The most stable isomer is followed by isomers 1643 (C_1), 1687 (C_1), 1644 (C_2), 1648 (C_1), 1686 (C_2), 1025 (C_1), 1646 (C_1), 1779 (C_2), 1769 (C_1), 1062 (C_1), 1078 (D_3), 574 (C_1), 1735 (S_4), 1765 (C_2), 206 (D_{3h}), in different orders depending on the used theoretical level [6, 7].

Nevertheless, several isomers of fullerene C_{108} have been identified as various derivatives (exohedral and endohedral). The most stable isomer 1771 (D_2) is identified as chloro derivative $C_{108}Cl_{12}$ by single-crystal X-ray analysis with the use of synchrotron radiation resulted in the structure determination and represents so far the largest pristine fullerenes with known cages [22]. Isomer 1660 (C_1) has been very recently characterized by X-ray diffraction as endohedral carbide metallofullerenes $Y_2C_2@C_{108}$ representing the largest metallofullerene that have been characterized by crystallography to date [23]. This giant species have been studied theoretically using the density functional theory (DFT), and even the MP2 technique, in order to supply further structure and stability data [24].

Thus, from 450 and 1799 IPR isomers for fullerenes C_{100} and C_{108}, respectively, no one isomer has been isolated and characterized as an empty cage so far. Nevertheless, several isomers of them have been stabilized and identified as various exohedral and endohedral derivatives. In this report, we present the study of the molecular structures of IPR isomer 450 (D_5) of C_{100} fullerene that is one of the most unstable isomers but stabilized as endohedral fullerenes $La_2@C_{100}$, $La_2C_2@C_{100}$, and, presumably, $Dy_2@C_{100}$ and IPR isomer 1771 (D_2) of C_{108} fullerene that is one of the most stable to establish their structures, reasons of instability, and their stabilization as various derivatives.

Methodology

Previously, we have developed an approach for studying the higher fullerenes that provides a complete structural formula of fullerene with the distribution of single, double, and π-delocalized bonds prior to the quantum-chemical calculations. We considered the substructures existing in the most stable fullerene molecules, for example, corannulene in C_{60} or indacene substructures in C_{70}, as a factor which does not reduce the molecular stability of any fullerene. On the contrary, the presence of large substructures consisting only of hexagons is the reason for significant local strains in fullerene molecule, and radical substructures are the reasons of the instability of such fullerenes. In fact, the analysis of all IPR molecular structures of higher fullerenes, such as C_{72}, C_{74}, C_{76}, C_{80}, C_{82}, C_{84}, C_{86} [25–29 and references therein], and some small fullerenes, such as C_{40} and C_{50} [30–32], confirmed this assumption.

The distribution of bonds in researched IPR isomers was carried out in accordance with the following rules: (i) pentagons consist only of single bonds, while in hexagons there is an alternation of single and double bonds; (ii) according to symmetry requirement, the hexagon with delocalized pi-bonds can be implemented; (iii) the distribution of the bonds should not lower the fullerene molecular symmetry; (iv) corannulene and indacene substructures, characteristic for the most stable fullerene C_{60} and C_{70}, are preferred.

The molecular structures of the investigated IPR isomers were fully optimized using DFT B3LYP functional [33, 34] with the 6-31G basis. At the first step, geometry optimization was performed without symmetry constraints. The calculations showed that in all cases, except for singlet and quintet configurations of isomer 450 (D_5) of fullerene C_{100}, the equilibrium geometries corresponded to the topological molecular symmetry of each isomer. Therefore, subsequent optimizations were carried out with the corresponding symmetry constraints. The standard keywords in the Gaussian package were used in optimization processes. To improve energies, geometry optimizations were followed by single-point calculations at the 6-31G* level. The calculations showed a good agreement between the results obtained for all used basis sets.

The isomer 450 (D_5) of fullerene C_{100} was considered with the open-shell electronic structure; the quantum-chemical calculations were carried out in triplet, quintet, and septet

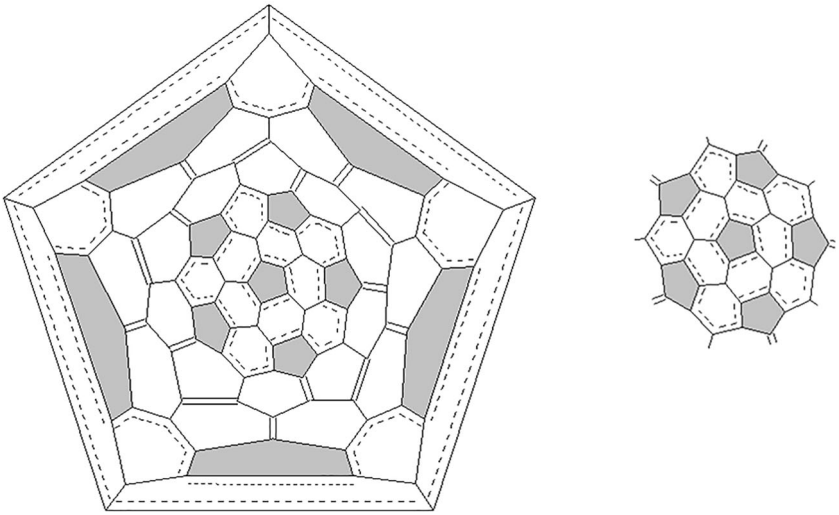

Fig. 1 Schlegel diagram of the IPR isomer 450 (D_5) of fullerene C_{100} (left) and substructure from five condensed phenalenyl-radicals—othrene (right)

configurations using unrestricted Kohn-Sham methodology. To ensure the calculated structures correspond to minima, vibrational analyses were performed at the same level of theory. The tests of the stability of wave functions were carried out. All calculations were performed using the GAUSSIAN16 program [35].

Results and discussion

Analysis of bond distribution in the isomer 450 (D_5) of fullerene C_{100} (Fig. 1, left) revealed that it contains two substructures with five condensed phenalenyl-radicals at the poles of the molecule that we named as othrene (Fig. 1, right). Phenalenyl substructure is known as a radical because all three bonds that radiate from the central carbon atom of this substructure must be equivalent according to molecular symmetry. Therefore, the carbon atom located on the third-order symmetry axis is considered to have one unpaired electron. This situation is similar to radical-fullerene C_{74} (D_{3h}) [27, 36] which has two phenalenyl-radical substructures on the C_3 axis of a molecule passing through the central carbon atom. Interestingly, two similar substructures with five condensed phenalenyl-radicals (othrene substructures) at the poles of the molecule were previously found in the IPR isomer 31923 (D_{5h}) of C_{80} fullerene [37]. It was shown that this IPR isomer cannot be isolated experimentally due to its radical nature [37]. Noteworthy is the presence of the equatorial belt from 20 condensed hexagons. So, according to an analysis of bond distribution, the isomer 450 (D_5) of fullerene C_{100} has an open-shell electronic structure.

The isomer 1771 (D_2) of fullerene C_{108} (Fig. 2, left) contains four corannulene and four s-indacene substructures that are stable like in C_{70} (D_{5h}) fullerene. Additionally, analysis of bond distribution allowed to reveal two substructures with two condensed coronene at the equator of the molecule (Fig. 2, right). The pair of coronene substructures of C_{72} is the reason for high local strains because this substructure tends to be planar, whereas a fullerene cage is close to spherical [25, 26]. However, it seems quite evident that the presence of coronene substructures becomes less critical when molecular size increases. Nevertheless, in our opinion, the presence of a

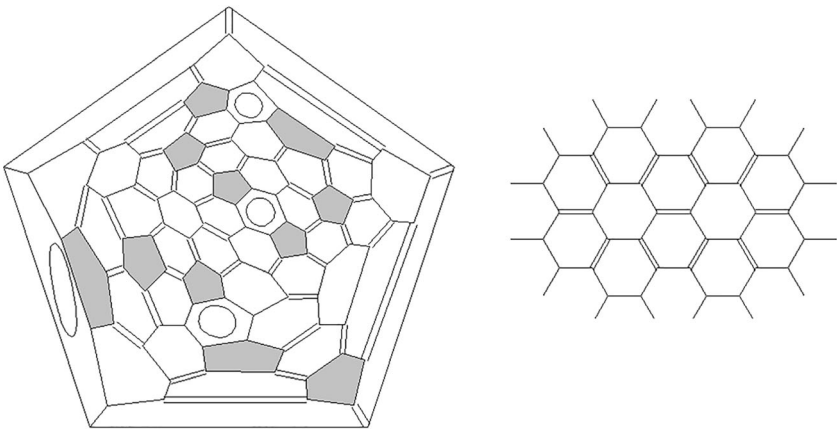

Fig. 2 Schlegel diagram of the IPR isomer 1771 (D_2) of the fullerene C_{108} (left) and substructure from two condensed coronenes (right)

Table 1 Relative energies (ΔE, kcal/mol) and HOMO-LUMO gaps (eV) of isomer 450 (D_5) of fullerene C_{100} and isomer 1771 (D_2) of fullerene C_{108}

Isomer no.	E		HOMO-LUMO	
	6-31G	6-31G*	6-31G	6-31G*
C_{100}, 450 (D_5) singlet (C_2)	0.87	0.57	0.67	0.67
triplet	0.00	0.00	0.70	0.70
quintet (C_2)	10.95	10.01	0.25	0.28
septet	21.87	20.82	0.24	0.28
C_{108}, 1771 (D_2) singlet	0.00	0.00	1.61	1.58
triplet	20.38	20.38	0.15	0.13

flat substructure with two condensed coronenes should introduce local strain even into a large molecule. In addition, both substructures of the "fused" coronenes are connected by two pairs of hexagons forming a belt consisting of 28 hexagons, which also introduces significant local strain. Thus, an analysis of bond distribution shows that this isomer has a closed shell without any radical centers with unpaired electrons, and the instability of this isomer is supposedly associated with high local strain.

DFT calculations predict the lowest energy for the triplet configuration of isomer 450 (D_5) of fullerene C_{100}, whereas isomer 1771 (D_2) of the fullerene C_{108} has a closed electronic shell (Table 1). It agrees with our tentative structural estimations. A symmetry-lowering distortion for singlet and quintet electronic configurations of isomer 450 (D_5) of fullerene C_{100} was founded. For triplet and septet configurations with 2 and 6 unpaired electrons, respectively, the D_5 symmetry is maintained; therefore, further, only these configurations were analyzed.

The open shell nature of isomer 450 (D_5) of fullerene C_{100} is additionally confirmed by the tests of the wave function stability. For the singlet states, computations predict RHF-to-UHF instability, suggesting the existence of state with lower energy. The wave functions of triplet, quintet, and septet states are stable under the considered perturbations.

The preliminary assumed bond distributions according to the developed approach are confirmed in DFT calculations: calculated bond lengths correspond to single, double, and delocalized pi-bonds plotted on Schlegel diagrams and are also in agreement with the well-known experimental values for most stable C_{60} and C_{70} fullerenes [38, 39] (Table 2 and Table S1 in Supporting Information).

However, the calculations revealed some deviations of the bond lengths from those expected during the bond distribution analysis by the developed approach: in particular, instead of some double bonds, the calculation shows the bond lengths, which should be classified as single (see max values of double bonds in Table 2 and Table S1 in Supporting Information). The analysis shows these discrepancies concern the bonds in the equatorial belt from 20 and 28 condensed hexagons in isomer 450 (D_5) of fullerene C_{100} and isomer 1771 (D_2) of fullerene C_{108}, respectively. It should be mentioned that such bond length distribution was found for the nanotubes [40, 41]. This circumstance should probably be considered when analyzing large fullerene molecules with fragments where pentagons are completely absent.

Previously, it has been shown that high distortion of fullerene cage, i.e., high nonplanarity of hexagons and pentagons causing a local strain in a fullerene molecule, is directly connected with its thermodynamic instability [26, 37, 42–46]. The most stable fullerene C_{60} molecule contains all planar hexagons and pentagons [38], whereas in the C_{70} molecule some distortions of hexagons and pentagons appear, with highest nonplanarity in hexagons with delocalized π-bond [47]. Such distortions of higher fullerene molecules are probably caused by the compensation of π-delocalization of hexagons embedded in a sphere-like fullerene cage. The analysis of molecular geometries of the fullerenes under study shows that there are no flat hexagons and pentagons in their structures (Fig. 3, Table 3). In contrast to C_{70}, maximum distortions are observed in hexagons with bond alternation (see Table 3). This suggests the presence of substantial local molecular strains in both studied fullerene molecules. The analysis of the localization of the most distorted cycles (with the

Table 2 The shortest and the longest bond lengths (Å) of isomer 450 (D_5) of fullerene C_{100} and isomer 1771 (D_2) of fullerene C_{108}

Isomer no.	Single		Double		Delocalized	
	Min	Max	Min	Max	Min	Max
C_{60} [38]	1.458		1.401		-	
C_{70}*	1.463		1.375		1.418	
C_{100}, 450 (D_5) triplet	1.4210	1.4737	1.3914	1.4503	1.4178	1.4534
septet	1.4262	1.4655	1.3979	1.4489	1.4156	1.4419
C_{108}, 1771 (D_2) singlet	1.4285	1.4766	1.3681	1.4510	1.4082	1.4377

*Calculated by us basing on X-ray data [39]

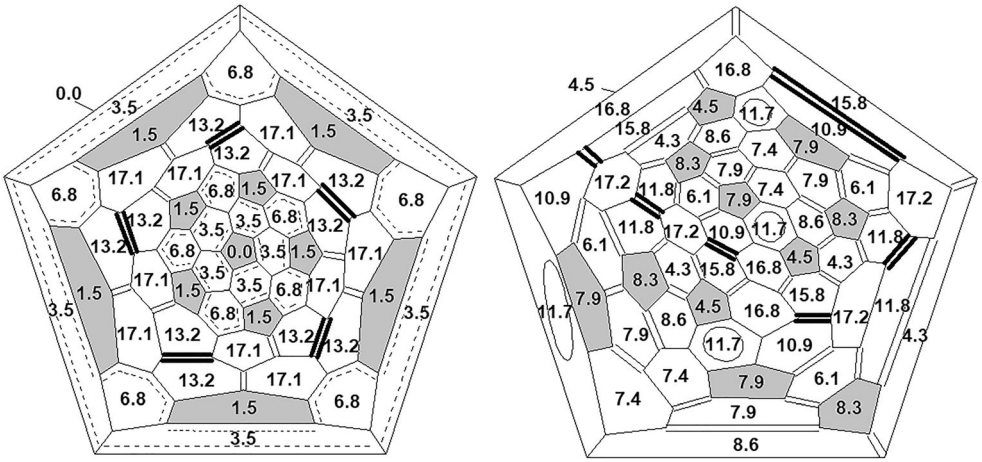

Fig. 3 Schlegel diagrams with maximal dihedral angles (degree) in cycles in isomer 450 (D_5) of fullerene C_{100} (left) and isomer 1771 (D_2) of the fullerene C_{108} (right)

maximum dihedral angles in a cycle) shows that they contain the elongated double bonds (see Fig. 3, depicted by bold).

A comparative analysis of dihedral angles between cycles (between hexagons, between pentagon and hexagon) in studied fullerenes and strained molecules of isomers 1 (D_2), 2 (C_2), and 20 (T_d) of fullerene C_{84} [42, 44, 48] shows that dihedral angles in these molecules are comparable (Table 4) that also indicates the presence of significant local strains in the molecules of studied fullerenes.

The spin density in the triplet and septet configurations of isomer 450 (D_5) of fullerene C_{100} is mainly concentrated on atoms of central pentagons of othrene radical substructures (Fig. 4 and Table S2 in Supporting Information). Analysis of DFT results revealed that configuration with 6 unpaired electrons (septet) is most preferred that is rationalized by the fact that part of the spin density in triplet configuration is outside of the othrene substructures, whereas in septet configuration the spin density is concentrated in the othrene substructures. The spin density distribution predetermines the position of the metal atom(s) inside the possibly synthesized in the future endohedral derivative or the order of radical addition in reactions of synthesis of exohedral derivatives. Really, DFT calculations of dimetallofullerenes $M_2@C_{100}$ (M = La, Y, Sc, Dy) show that metal atoms in these endohedral dimetallofullerenes are located near poles of molecules [14, 15, 17]. Authors explain such metal atom's positions by the longest metal-metal distances to minimize the electrostatic repulsion between them [15]. However, in our opinion, the positions of metal atoms are determined by the initial structure of the fullerene with the presence of radical centers at the poles of the molecule and the corresponding distribution of spin density.

Analysis of the chlorination pattern of C_{108}-1771(C_2)Cl_{12} shows that 12 chlorine atoms are unequally distributed on the C_{108} cage [22]. Usually, the most stable addition patterns of the derivatives with 12 atoms or groups are characterized by their uniform distribution on the fullerene cages [22]. Authors explain such deviations from the general rule by the formation of stabilizing substructures on the carbon cages such as benzenoid rings or isolated C=C bonds. Our combined analysis of the initial molecule structure and experimental data on the chlorine addend distribution [22] reveals that 8 of 12 addends attached by pairs to all four hexagons with delocalized π-bonds (Fig. 5). Such an attachment is most advantageous from the point of view of minimal rearrangement of the entire electronic system of the molecule. So, analysis of chlorination pattern confirmed our earlier conclusion [49] about the preference of hexagons with delocalized π-bonds as the most feasible positions of addend in radical addition reaction.

Table 3 Maximal dihedral angles (degree) in isomer 450 (D_5) of fullerene C_{100} and isomer 1771 (D_2) of fullerene C_{108}

Isomer no.	In hexagons with		In pentagons
	bond alternation	delocalized π-bonds	
C_{100}, 450 (D_5) triplet	16.77 (10)	6.66 (10)	1.32 (10)
septet	17.07 (10)	6.82 (10)	1.55 (10)
C_{108}, 1771 (D_2) singlet	17.19 (4)	11.71 (4)	8.27 (4)

*Numbers in parentheses represent the number of equivalent cycles according to the isomer symmetry

Table 4 Dihedral angles between hexagons (HH) and between pentagon and hexagon (PH) in isomer 450 (D_5) of fullerene C_{100} and isomer 1771 (D_2) of fullerene C_{108} and locally strained molecules of isomers 1 (D_2), 2 (C_2), and 20 (T_d) of fullerene C_{84}

Isomer no.	HH	PH
C_{100}, 450 (D_5) triplet	140.49[a]	144.12
	174.04	152.18
C_{100}, 450 (D_5) septet	140.11	144.41
	174.25	152.25
C_{108}, 1771 (D_2) singlet	138.64	136.19
	174.45	154.05
Fullerene C_{84}[b]		
Isomer 1 (D_2)	127.05	124.27
	173.66	161.89
Isomer 2 (C_2)	128.69	125.31
	170.84	161.75
Isomer 20 (T_d)	138.23	133.19
	156.33	157.72

[a] Minimum and maximum values, respectively

[b] From Ref. [42, 44, 48]

Thus, the instabilities of the studied fullerenes are caused by the significant local strains due to the presence of substructures consisting of condensed hexagons for both researched fullerenes and additionally by open-shell electronic structure for isomer 450 (D_5) of fullerene C_{100}. It means they should be unstable and probably could not be obtained as empty molecules. However, they can be stabilized in polymeric form and as exohedral or endohedral derivatives. It is shown that application of the developed approach in combination with quantum chemical calculations can be successfully used for determining the structure of molecules of higher fullerenes with the number of carbon atoms greater than 90 which is useful to obtain such information by experimental methods.

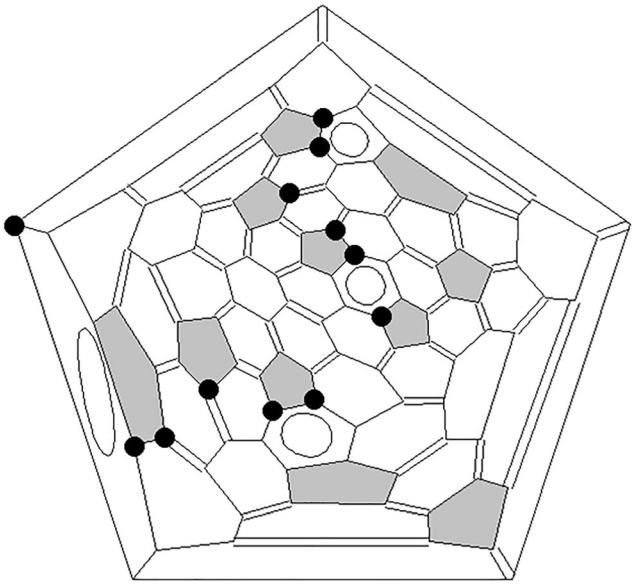

Fig. 5 The initial structure of isomer 1771 (D_2) of fullerene C_{108} together with the position of addends in C_{108}-1771(C_2)Cl_{12} according to [22] (black circles denote the positions of attached Cl atoms)

Conclusions

An analysis of the molecular structures of IPR isomer 450 (D_5) of fullerene C_{100} and IPR isomer 1771 (D_2) of fullerene C_{108} was carried out. The data about the distributions of single, double, and delocalized π-bonds in studied isomer molecules as well as their molecular formulas are presented for the first time. It is revealed that isomer 450 (D_5) of fullerene C_{100} contains two substructures from condensed phenalenyl-radicals at the poles of the molecule (i.e., has an open electronic shell), whereas isomer 1771 (D_2) of fullerene C_{108} has a closed electronic shell and contains a substructure from condensed coronenes at the equator of the molecule. Their stabilities are evaluated in accordance with local strains in the molecules and/or the presence of radical substructures. The most probable positions of addends in the products of radical addition are shown.

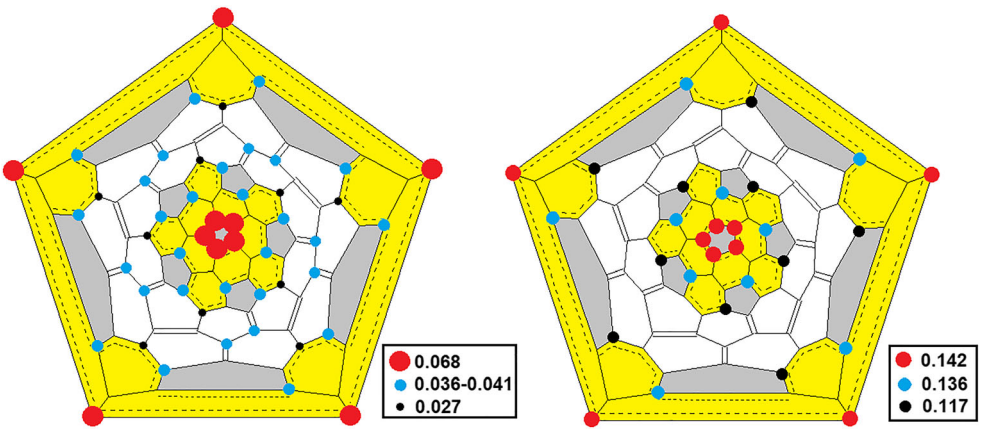

Fig. 4 The spin density distribution (marked by bold circles in accordance with their values from 0.03 to 0.14) in the triplet (left) and septet (right) configurations of isomer 450 (D_5) of fullerene C_{100}; regions with maximum spin densities are depicted by yellow

Supplementary Information The online version contains supplementary material available at https://doi.org/10.1007/s11224-021-01803-0.

Code availability N/A.

Author contribution The manuscript was written with contributions from all authors. All authors have approved the final version of the manuscript.

Funding This work received financial support from the government assignment for FRC Kazan Scientific Center of RAS and was partially supported by the Russian Foundation for Basic Research under Grant No.18-29-19110mk.

Data availability All data generated or analyzed during this study are included in this published article (and its supplementary information files).

Declarations

Ethics approval N/A.

Consent to participate N/A.

Consent for publication N/A.

Conflict of interest The authors declare no competing interests.

References

1. Kroto HW (1987) The stability of the fullerenes Cn, with n = 24, 28, 32, 36, 50, 60 and 70. Nature 329:529–531. https://doi.org/10.1038/329529a0
2. Schmalz TG, Seitz WA, Klein DJ, Hite GE (1988) Elemental carbon cages. J Am Chem Soc 110:1113–1127. https://doi.org/10.1021/ja00212a020
3. Fowler PW, Manolopoulos DE (2007) An atlas of fullerenes. Dover Publ, Mineola, NY, USA
4. Zhang BL, Wang CZ, Ho KM, Xu CH, Chan CT (1993) The geometry of large fullerene cages C_{72} to C_{102}. J Chem Phys 98:3095–3102. https://doi.org/10.1063/1.464084
5. Zhao X, Goto H, Slanina Z (2004) C_{100} IPR fullerenes: temperature-dependent relative stabilities based on the Gibbs function. Chem Phys 306:93–104. https://doi.org/10.1016/j.chemphys.2004.07.019
6. Cai WS, Xu L, Shao N, Shao XG, Guo QX (2005) An efficient approach for theoretical study on the low-energy isomers of large fullerenes C_{90}–C_{140}. J Chem Phys 122:184318. https://doi.org/10.1063/1.1891706
7. Shao N, Gao Y, Yoo S, An W, Zeng XC (2006) Search for lowest-energy fullerenes: C_{98} to C_{110}. J Phys Chem A 110:7672–7676. https://doi.org/10.1021/jp0624092
8. Wang D, Yu H, Sun X, Hou D (2011) Theoretical study on C_{100} fullerenes and $C_{96}X_4$ (X = N, P, B, Si). Physica B 406:1233–1237. https://doi.org/10.1016/j.physb.2011.01.004
9. Fritz MA, Kemnitz E, Troyanov SI (2014) Capturing an unstable C_{100} fullerene as chloride, $C_{100}(1)Cl_{12}$, with a nanotubular carbon cage. Chem Commun 50:14577–14580. https://doi.org/10.1039/c4cc06825d
10. Wang S, Yang S, Kemnitz E, Troyanov SI (2016) New Isolated-Pentagon-Rule and skeletally transformed isomers of C_{100} fullerene identified by structure elucidation of their chloro derivatives. Angew Chem Int Ed 55:3451–3454. https://doi.org/10.1002/anie.201511928
11. Fanhua Y, Kai T (2018) Density Functional Theory study on the formation mechanism of Isolated-Pentagon-Rule $C_{100}(417)Cl_{28}$. Acta Phys -Chim Sin 34(3):256–262. https://doi.org/10.3866/PKU.WHXB201708071
12. Yang S, Wang S, Kemnitz E, Troyanov SI (2014) Chlorination of IPR C_{100} fullerene affords unconventional $C_{96}Cl_{20}$ with a nonclassical cage containing three heptagons. Angew Chem Int Ed 53:2460–2463. https://doi.org/10.1002/anie.201310099
13. Ioffe IN, Yang S, Wang S, Kemnitz E, Sidorov LN, Troyanov SI (2015) C_{100} is converted into $C_{94}Cl_{22}$ by three chlorination-promoted C_2 losses under formation and elimination of cage heptagons. Chem Eur J 21:4904–4907. https://doi.org/10.1002/chem.201406487
14. Yang T, Zhao XA, Nagase S (2011) Di-lanthanide encapsulated into large fullerene C_{100}: a DFT survey. Phys Chem Chem Phys 13:5034–5037. https://doi.org/10.1039/c0cp01840f
15. Mu L, Bao X, Yang S, Kong X (2017) Dimetallofullerene $M_2@C_{100}$ or carbide cluster fullerene $M_2C_2@C_{98}$ (M = La, Y, and Sc): which ones are more stable? RSC Adv 7:16149–16154. https://doi.org/10.1039/c7ra00717e
16. Beavers CM, Jin H, Yang H, Wang Z, Wang X, Ge H, Liu Z, Mercado BQ, Olmstead MM, Balch AL (2011) Very large, soluble endohedral fullerenes in the series La_2C_{90} to La_2C_{138}: isolation and crystallographic characterization of $La_2@D_5(450)$-C_{100}. J Am Chem Soc 133:15338–15341. https://doi.org/10.1021/ja207090e
17. Cai W, Bao L, Zhao S, Xie Y, Akasaka T, Lu X (2015) Anomalous compression of $D_5(450)$-C_{100} by encapsulating La_2C_2 cluster instead of La_2. J Am Chem Soc 137:10292–10296. https://doi.org/10.1021/jacs.5b05668
18. Yang SF, Dunsch L (2006) Di-and tridysprosium endohedral metallofullerenes with cages from C_{94} to C_{100}. Angew. Chem. Int Ed 45:1299–1302. https://doi.org/10.1002/anie.200502417
19. Valencia R, Rodriguez-Fortea A, Poblet JM (2007) Large fullerenes stabilized by encapsulation of metallic clusters. Chem Commun: 4161–4163. https://doi.org/10.1039/B709548A
20. Rodriguez-Fortea A, Alegret N, Balch AL, Poblet JM (2010) The maximum pentagon separation rule provides a guideline for the structures of endohedral metallofullerenes. Nat Chem 2:955–961. https://doi.org/10.1038/nchem.837
21. Rodriguez-Fortea A, Balch AL, Poblet JM (2011) Endohedral metallofullerenes: a unique host-guest association. Chem Soc Rev 40:3551–3563. https://doi.org/10.1039/c0cs00225a
22. Wang S, Yang S, Kemnitz E, Troyanov SI (2016) New giant fullerenes identified as chloro derivatives: Isolated-Pentagon-Rule $C_{108}(1771)Cl_{12}$ and $C_{106}(1155)Cl_{24}$ as well as nonclassical $C_{104}Cl_{24}$. Inorg Chem 55:5741–5743. https://doi.org/10.1021/acs.inorgchem.6b00809
23. Pan C, Bao L, Yu X, Fang H, Xie Y, Akasaka T, Lu X (2018) Facile access to Y_2C_{2n} (2n = 92-130) and crystallographic characterization of $Y_2C_2@C_1(1660)$-C_{108}: a giant nanocapsule with a linear carbide cluster. ACS Nano 12:2065–2069. https://doi.org/10.1021/acsnano.8b00384
24. Slanina Z, Uhlík F, Pan C, Akasaka T, Lu X, Adamowicz L (2018) Computed stabilization for a giant fullerene endohedral: $Y_2C_2@C_1(1660)$-C_{108}. Chem Phys Lett 710:147–149. https://doi.org/10.1016/j.cplett.2018.08.051
25. Kovalenko VI, Khamatgalimov AR (2006) Regularities in the molecular structure of stable fullerenes. Russ Chem Rev 75(11):981–988. https://doi.org/10.1070/RC2006v075n11ABEH003620
26. Khamatgalimov AR, Kovalenko VI (2016) Structures of unstable Isolated-Pentagon-Rule fullerenes C_{72}-C_{86} molecules. Russ Chem Rev 85(8):836–853. https://doi.org/10.1070/RCR4571
27. Khamatgalimov AR, Kovalenko VI (2018) Radical IPR fullerenes C_{74} (D_{3h}) and C_{76} (T_d): dimer, trimer, etc. Experiments and theory.

J Phys Chem C 122(5):3146–3151. https://doi.org/10.1021/acs.jpcc.7b11940
28. Khamatgalimov AR, Melle-Franco M, Gaynullina AA, Kovalenko VI (2019) Ythrene: from the real radical fullerene substructure to hypothetical (yet?) radical molecules. J Phys Chem C 123(3):1954–1959. https://doi.org/10.1021/acs.jpcc.8b10526
29. Khamatgalimov AR, Kovalenko VI (2021) Substructural approach for assessing the stability of higher fullerenes. Int J Mol Sci 22(7):3760. https://doi.org/10.3390/ijms22073760
30. Khamatgalimov AR, Idrisov RI, Kamaletdinov II, Kovalenko VI (2020) The key feature of instability of small non-IPR closed-shell fullerenes: three isomers of C_{40}. Mendeleev Commun 30:725–727. https://doi.org/10.1016/j.mencom.2020.11.012
31. Khamatgalimov AR, Yakupova LI, Kovalenko VI (2020) Features of molecular structure of small non-IPR fullerenes: the two isomers of C_{50}. Theor Chem Accounts 139:1–8. https://doi.org/10.1007/s00214-020-02675-z
32. Khamatgalimov AR, Idrisov RI, Kamaletdinov II, Kovalenko VI (2021) Open-shell nature of non-IPR fullerene C_{40}: isomers 29 (C_2) and 40 (T_d). J Mol Model 27:22. https://doi.org/10.1007/s00894-020-04625-9
33. Becke AD (1993) Density-functional thermochemistry. III The role of exact exchange J Chem Phys 98:5648–5652. https://doi.org/10.1063/1.464913
34. Lee C, Yang W, Parr RG (1988) Development of the Colle-Salvetti correlation-energy formula into a functional of the electron density. Phys Rev B 37:785–789. https://doi.org/10.1103/PhysRevB.37.785
35. Frisch MJ, Trucks GW, Schlegel HB, Scuseria GE, Robb MA, Cheeseman JR, Scalmani G, Barone V, Petersson GA, Nakatsuji H, Li X, Caricato M, Marenich AV, Bloino J, Janesko BG, Gomperts R, Mennucci B, Hratchian HP, Ortiz JV, Izmaylov AF, Sonnenberg JL, Williams-Young D, Ding F, Lipparini F, Egidi F, Goings J, Peng B, Petrone A, Henderson T, Ranasinghe D, Zakrzewski VG, Gao J, Rega N, Zheng G, Liang W, Hada M, Ehara M, Toyota K, Fukuda R, Hasegawa J, Ishida M, Nakajima T, Honda Y, Kitao O, Nakai H, Vreven T, Throssell K, Montgomery JA, Peralta JE, Ogliaro F, Bearpark MJ, Heyd JJ, Brothers EN, Kudin KN, Staroverov VN, Keith TA, Kobayashi R, Normand J, Raghavachari K, Rendell AP, Burant JC, Iyengar SS, Tomasi J, Cossi M, Millam JM, Klene M, Adamo C, Cammi R, Ochterski JW, Martin RL, Morokuma K, Farkas O, Foresman JB, Fox DJ (2016) Gaussian 16, revision B.01. Gaussian, Inc., Wallingford, CT
36. Kovalenko VI, Khamatgalimov AR (2003) Open-shell fullerene C_{74}: phenalenyl-radical substructures. Chem Phys Lett 377:263–268. https://doi.org/10.1016/S0009-2614(03)01055-8
37. Khamatgalimov AR, Kovalenko VI (2011) Electronic structure and stability of C_{80} fullerene IPR isomers. Fuller Nanotub Car Nanostruct 19:599–604. https://doi.org/10.1080/1536383X2010504951
38. Hedberg K, Hedberg L, Bethune DS, Brown CA, Dorn HC, Johnson RD, de Vries M (1991) Bond lengths in free molecules of buckminsterfullerene, C_{60}, from gas-phase electron diffraction. Science 254:410–412. https://doi.org/10.1126/science2545030410
39. Hedberg K, Hedberg L, Buhl M, Bethune DS, Brown CA, Johnson RD (1997) Molecular structure of free molecules of the fullerene C_{70} from gas-phase electron diffraction. J Am Chem Soc 119:5314–5329. https://doi.org/10.1021/ja970110e
40. Imtani AN (2009) Jindal VK. Characterizing single-walled carbon nanotubes by pressure probe Carbon 47:3247–3251. https://doi.org/10.1016/jcarbon200907041
41. Tuktamysheva RA, Khamatgalimov AR, Kovalenko VI (2014) Electronic and geometric structures of some isomers of fullerene C_{90} and the structures of their chlorides and perfluoroalkyl polyadducts. Butlerov Comm 37:1–12
42. Khamatgalimov AR, Luzhetskii AV, Kovalenko VI (2008) Unusual pentagon and hexagon geometry of three isomers (no 1, 20, and 23) of fullerene C_{84}. Int J Quantum Chem 108:1334–1339. https://doi.org/10.1002/qua21638
43. Khamatgalimov AR, Kovalenko VI (2011) Electronic structure and stability of fullerene C_{82} IPR isomers. J Phys Chem A 115:12315–12320. https://doi.org/10.1021/jp204565q
44. Khamatgalimov AR, Kovalenko VI (2012) 24 IPR isomers of fullerene C_{84}: cage deformation as geometrical characteristic of local strains. Int J Quantum Chem 112:1055–1065. https://doi.org/10.1002/qua23099
45. Khamatgalimov AR, Kovalenko VI (2015) Stability of Isolated-Pentagon-Rule isomers of fullerene C_{76}. Fuller Nanotub Car Nanostruct 23:148–152. https://doi.org/10.1080/1536383X2012758114
46. Khamatgalimov AR, Kovalenko VI (2017) Molecular structures of the open-shell IPR isomers of fullerene C_{90}. Fuller Nanotub Car Nanostruct 25:179–184. https://doi.org/10.1080/1536383X20161277992
47. Zverev VV, Kovalenko VI (2006) An analysis of the structure of fullerene C_{70} by quantum-chemical methods. Russ J Phys Chem 80:99–105. https://doi.org/10.1134/S003602440601016X
48. Khamatgalimov AR, Kovalenko VI (2010) Deformation and thermodynamic instability of a C_{84} fullerene cage. Russ J Phys Chem A 84:636–641. https://doi.org/10.1134/S0036024410040205
49. Khamatgalimov AR, Kovalenko VI (2017) Stabilization of higher IPR fullerenes C_{74} (D_{3h}) and C_{76} (T_d) with open shell in radical addition reactions. Fuller Nanotub Car Nanostruct 25(2):128–132. https://doi.org/10.1080/1536383X20161269320